Human Pathology (2018) 79, 1–8

ELSEVIER

Human PATHOLOGY

www.elsevier.com/locate/humpath

In this issue

Analysis of cancer-associated fibroblasts and the epithelial-mesenchymal transition in cutaneous basal cell carcinoma, squamous cell carcinoma, and malignant melanoma☆,☆☆

Kousuke Sasaki MD[a,b], Tamotsu Sugai MD[a,*], Kazuyuki Ishida MD[a], Mitsumasa Osakabe MD[a], Hiroo Amano MD[c], Hiroaki Kimura MD[b], Minoru Sakuraba MD[b], Katsuhiko Kashiwa MD[b], Seiichiro Kobayashi MD[b]

[a]*Department of Molecular Diagnostic Pathology, School of Medicine, Iwate Medical University, Morioka 020-8505, Japan*
[b]*Department of Plastic Surgery, School of Medicine, Iwate Medical University, Morioka 020-8505, Japan*
[c]*Department of Dermatology, School of Medicine, Iwate Medical University, Morioka 020-8505, Japan*

Received 21 December 2017; revised 5 March 2018; accepted 7 March 2018

Keywords:
Cancer-associated fibroblast (CAF);
CAF phenotype;
Cutaneous cancer;
Epithelial-mesenchymal transition;
Immunohistochemistry

Summary Activated cancer-associated fibroblasts (CAFs) and fibroblasts that have undergone the epithelial-mesenchymal transition (EMT) in cancer stroma contribute to tumor progression and metastasis. However, no reports have investigated the CAF phenotype and its clinicopathological relevance in cutaneous malignant tumors, including basal cell carcinoma (BCC), squamous cell carcinoma (SCC), and malignant melanoma (MM). Here, we investigated the CAF phenotype in cutaneous malignant tumors based on their histology and immunohistochemical expression of CAF-related markers, including adipocyte enhancer–binding protein 1 (AEBP1), podoplanin, platelet-derived growth factor receptor α (PDGFRα), PDGFRβ, fibroblast activating protein (FAP), CD10, S100A4, α-smooth muscle actin (α-SMA), and EMT-related markers (Zeb1, Slug, and Twist). In addition, we assessed the role of the CAF phenotype in cutaneous malignant cancers using hierarchical cluster analysis. Consequently, 3 subgroups were stratified based on the expression pattern of CAF- and EMT-related markers. Subgroup 1 was characterized by low expression of AEBP1, PDGFRα, PDGFRβ, FAP and Slug, whereas subgroup 2 was closely associated with high expression of PDGFRβ, S100A4 and Twist. In addition, high expression levels of podoplanin, PDGFRβ, CD10, S100A4, α-SMA, Zeb1, Slug and Twist were observed in subgroup 3. High expression of CD10 was commonly found in all 3 subgroups. These subgroups were correlated with histologic subtypes, that is, subgroup 1, MM; subgroup 2, BCC; and subgroup 3, SCC. We suggest that the expression pattern of CAF- and EMT-related proteins plays crucial roles in the progression of BCC, SCC, and MM.

☆ Kousuke Sasaki and Tamotsu Sugai contributed equally to this article.
☆☆ Disclosures: The authors declare no conflicts of interest. This study was not supported by any funding.
* Corresponding author at: Department of Molecular Diagnostic Pathology, Iwate Medical University, 19-1, Morioka 020-8505, Japan.
E-mail address: tsugai@iwate-med.ac.jp (T. Sugai).

https://doi.org/10.1016/j.humpath.2018.03.006

1. Introduction

Basal cell carcinoma (BCC), squamous cell carcinoma (SCC), and malignant melanoma (MM) are the most frequent cutaneous malignant tumors, the incidence of which has been increasing [1]. The 3 malignant tumors share common properties in that the skin is habitually exposed to sunlight and there may be chronic ultraviolet-induced damage in cutaneous malignant tumors possibly followed by development of cutaneous BCC, SCC, and MM [2]. However, it is well accepted that the pathogeneses of the 3 cutaneous malignant tumors are different.

A previous study has shown that cutaneous SCC is primarily caused by multiple genetic mutations that enhance dysregulation of the cell cycle that is evoked by TP53 mutation [3]. BCC is also associated with genetic mutations that induce the proliferative activity of basal cells and is caused by uncontrolled activation of the hedgehog signal pathway. However, this disease is known to follow an innocent course that is different from the other 2 diseases (MM and SCC) [4]. Cutaneous melanoma cells display molecular alterations that are characterized by RAS-BRAF-MEK-ERK mitogen activation of the protein kinase signal pathway, consequently causing uncontrolled proliferation of the affected malignant melanocytes [5]. In addition, MM shows the worst outcome in patient survival. These findings suggest that the 3 cutaneous tumors (MM, BCC, and SCC) have different pathogenic courses, although they share common alterations.

Although tumors are composed of both cancer and stromal cells, studies of oncogenesis have generally focused on the cancer cells [6,7]. However, recent studies have shown that stromal cells surrounding the cancer nest play a major role in the progression and invasion of cancer [6,7]. The stromal cells, called "carcinoma-associated fibroblasts" (CAFs), promote oncogenesis and impair drug sensitivity [8,9]. The association of cancer cells with the surrounding CAFs is only partially understood. However, it is known that CAFs express various proteins constituting a heterogeneous range of phenotypes [10,11]. These findings support the idea that specific CAF phenotypes contribute to tumor progression. In fact, the specific phenotype of CAFs might influence the later behavior of cancer cells [12].

Recent data suggest that the metastatic process is not entirely linked to tumor growth, per se, but is controlled by other factors including the epithelial-mesenchymal transition (EMT), which allows cancer cells to dedifferentiate and acquire enhanced migratory and invasive properties [13,14]. The down-regulation of E-cadherin during the EMT seems to be mediated by transcriptional repression due to the binding of EMT transcription factors such as Zeb1, Slug, and Twist [15,16]. These EMT-related markers are also expressed in CAFs and may define their phenotype. We propose that improved understanding of the molecular pathogenesis underlying cutaneous malignant tumors can be achieved by analyzing EMT-related proteins in both CAFs and tumor cells. Here, we aimed to identify the role of CAF- and EMT-related proteins in cutaneous BCC, SCC, and MM. In addition, we attempted to show that different CAF phenotypes (defined by the expression pattern of various CAF- and EMT-related proteins) are present in BCC, SCC, and MM.

2. Materials and methods

2.1. Patients

A total of 237 formalin-fixed, paraffin-embedded tumor tissues were obtained from Iwate Medical University from 2009 to 2016. They included BCC, SCC, and MM. Clinicopathological findings of patients are summarized in Table 1, including sex, median age, median size, presence of solar keratosis, median tumor thickness, Clark level, and the presence of lymph node metastasis. All hematoxylin and eosin–stained slides were reviewed independently by 2 dermatopathologists (K. I. and T. S.). No patient received preoperative chemotherapy or radiotherapy.

Table 1 Clinicopathological findings in BCC, SCC, and MM examined

	Histologic classification (n = 237)		
	BCC (n = 110)	SCC (n = 87)	MM (n = 40)
Sex (man/woman)	50/60	39/48	20/20
Age (y), median (range)	75 (42-95)	81 (44-96)	76.5 (31-91)
Tumor size (mm), median (range)	12.2 (1.5-70.0)	25.0 (5.0-140.0)	20.0 (1.5-95.0)
Solar elastosis, positive (%)	87 (79.1)	55 (63.2)	13 (32.5)
Tumor thickness (mm), median (range)	2.0 (0.1-12.0)	4.5 (0.5-24.5)	3.6 (0.3-22.0)
Clark's level (%)			
I	0 (0)	0 (0)	0 (0)
II	9 (8.2)	6 (6.9)	3 (7.5)
III	18 (16.4)	6 (6.9)	9 (22.5)
IV	58 (52.7)	47 (54.0)	14 (35.0)
V	25 (22.7)	28 (32.2)	14 (35.0)
Lymph node metastasis, positive (%)	0 (0)	7 (8.0)	13 (32.5)

Table 2 Antibodies we used in the present study

Antibody	Company	Clone	Dilution	Activation method
AEBP1	Abcam (Cambridge, UK)	Ab54820	1:100	Heat retrieval pH 9, 20 min
Podoplanin	Dako (Glostrup, Denmark)	D2-40	1:100	Heat retrieval pH 9, 20 min
PDGFRα	Abcam (Cambridge, UK)	D13C6	1:200	Heat retrieval pH 9, 20 min
PDGFRβ	Abcam (Cambridge, UK)	Y62	1:100	Heat retrieval pH 9, 20 min
FAP	Abcam (Cambridge, UK)	Polyclonal	1:100	Heat retrieval pH 6, 20 min
CD10	Dako (Glostrup, Denmark)	56C6	1:100	Heat retrieval pH 9, 20 min
S100A4	Dako (Glostrup, Denmark)	Polyclonal	1:400	Heat retrieval pH 6, 20 min
α-SMA	Dako (Glostrup, Denmark)	1A4	1:100	Heat retrieval pH 9, 20 min
Slug	Cell Signaling (Danvers, Massachusetts, USA)	C19G7	1:50	Heat retrieval pH 9, 20 min
TWIST	Abcam (Cambridge, UK)	Twist2C1a	1:300	Heat retrieval pH 9, 20 min
ZEB1	Sigma-Albrich (St.Louis, Missouri, USA)	Polyclonal	1:200	Heat retrieval pH 6, 20 min

This study was approved by the Ethical Research Committee of Iwate Medical University.

2.2. Construction of tissue arrays

The tissues were fixed in 10% formalin and paraffin embedded according to routine procedures. Representative areas of tumors were assessed by hematoxylin and eosin staining of slides; a corresponding area was marked on the surface of the paraffin block. To examine protein expression immunohistochemically, we constructed 24 different tissue arrays containing the distinctive histologic types of the tumors. Each tissue array was constructed as previously described [17]. Briefly, two 1.5-mm-diameter cylinders of tissue were taken from representative areas of each archival paraffin block and arrayed into a new recipient paraffin block with a custom-built precision instrument (Beecher Instruments, Silver Spring, MD) according to the previously described method [17]. To evaluate each primary tumor, the invasive front was selected for cylinder core sampling. Initial sections were stained for hematoxylin and eosin to confirm the histopathological findings.

2.3. Immunohistochemistry

After deparaffinization and rehydration, the sections were heated in a microwave oven for 2 × 5 minutes in Tris-EDTA buffer (pH 9.0) and then incubated in a Tris-EDTA buffer for 20 minutes and washed twice for 5 minutes in phosphate-buffered saline. Hydrogen peroxide (5%, 5 minutes) was used to block endogenous peroxidase. Nonspecific binding was blocked with 1.5% normal serum in phosphate-buffered saline for 35 minutes at room temperature. The sections were incubated overnight at 4°C with the 11 monoclonal/polyclonal antibodies. The antibodies used in this study are listed in Table 2. Immunohistochemistry was carried out using the Dako Envision+ system, with dextran polymers conjugated with horseradish peroxidase (Dako (Glostrup, Denmark)), as previously described [18]. The specimens were heated in citrate buffer (pH 6.0) 3 times for 5 minutes each using a microwave (H2500, Microwave Processor; Bio-Rad, Hercules, CA) at 750 W before incubation with antibodies, as previously described. Hematoxylin was used as the counterstain.

2.4. Evaluation of CAF- and EMT-related markers

The stromal fibroblastic compartment of each tumor was examined for its immunopositivity for adipocyte enhancer–binding protein (AEBP1), podoplanin, platelet-derived growth factor receptor α (PDGFRα), PDGFRβ, fibroblast activating protein (FAP), CD10, S100A4, α-smooth muscle actin (α-SMA), Zeb1, Slug, and Twist. Inflammatory cells, such as histiocytes, were carefully excluded from the analysis. Digital pathology with Aperio ImageScope software (v12.3.2.5030 Leica Biosystems Inc., Buffalo Grove, Illinois, USA) was used to evaluate immunoexpression of AEBP1, podoplanin, PDGFRα, PDGFRβ, FAP, CD10, S100A4,α-SMA, Zeb1, Slug, Twist, and Zeb1. Only nuclear positivity for Zeb1, Twist, and Slug was considered significant, whereas only cytoplasmic expression of AEBP1, podoplanin, PDGFRα, PDGFRβ, FAP, CD10, S100A4, and α-SMA was regarded as positive. The immunostaining intensity and the involved area were examined separately. The immunostaining intensity for fusiform stromal cells was classified into 4 categories according to staining intensity as follows: negative, weak, moderate, and strong. The immunostaining area for fusiform stromal cells was semiquantified as follows: 0%, 0 to 20%, 20% to 50%, and 50% to 100%. The combination of intensity and area was scored (Table 3).

Table 3 Immunohistochemical scoring according to immunostaining intensity and area

Staining intensity	Staining area (%)			
	0	0 < area ≤ 20	20 < area ≤ 50	50 < area ≤ 100
Negative	Score 0	Score 0	Score 0	Score 0
Weak	Score 0	Score 1	Score 1	Score 2
Moderate	Score 0	Score 1	Score 2	Score 3
Strong	Score 0	Score 2	Score 3	Score 3

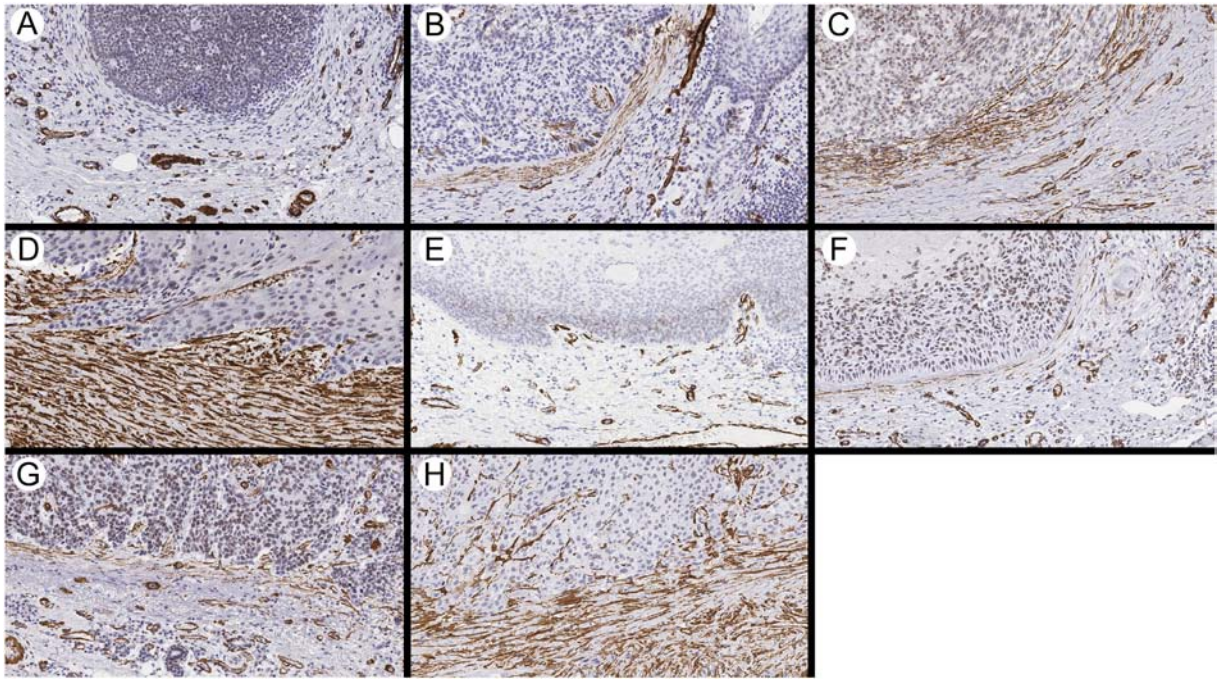

Fig. 1 Representative illustration of immunohistochemical intensity and area of α-SMA. Negative (A), weak (B), moderate (C), strong (D), 0 (E), 0 < area ≤20 (F), 20 < area ≤50 (G), 50 < area ≤100 (H). A–H, Original magnification ×20.

2.5. Hierarchical analysis of the expression of CAF and EMT markers

Tumor cells were individually scored as 0, 1+, 2+, and 3+ based on their cytoplasm/nuclear staining and intensity. Representative images are shown in Figures 1 and 2.

Hierarchical cluster analysis was performed for clustering of the samples according to the above scoring (0-3+) to achieve maximal homogeneity for each group and the greatest differences between the groups using open-access clustering software (Cluster 3.0 software; bonsai.hgc.jp/~mdehoon/software/cluster/software.htm). The clustering algorithm was set to centroid linkage clustering, which is the standard hierarchical clustering method used in biological studies.

2.6. Statistical analysis

Data were analyzed using JMP 10.0 software package (SAS Institute, Inc, Cary, NC). Data obtained for clinicopathological features (sex, macroscopic type, location, histologic

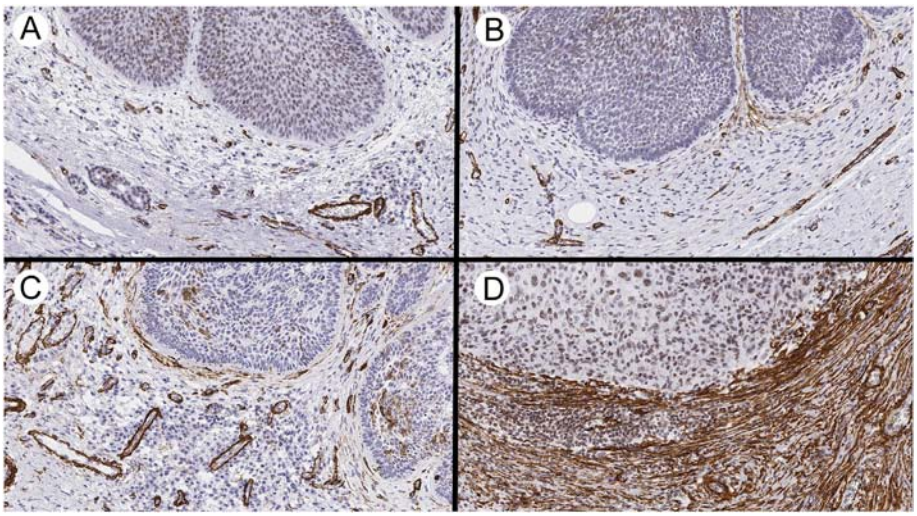

Fig. 2 Representative illustration of immunohistochemical score of α-SMA. A, Score 0 (intensity, negative; area, 0%). B, Score 1 (intensity, weak, and area, 20%). C, Score 2 (intensity, moderate; area, 40%). D, Score 3 (intensity, strong; area, 90%). A–D, Original magnification ×20.

type, classification of submucosal invasion, and lymph node metastasis) and immunohistochemical patterns of CAFs (ie, AEBP1, podoplanin, PDGFRα, PDGFRβ, FAP, CD10, S100A4, α-SMA, and EMT-related proteins [ie, Twist, Zeb1, and Slug]) based on each subgroup were analyzed using χ^2 tests.

For statistical analysis of the expression of AEBP1, podoplanin, PDGFRα, PDGFRβ, FAP, CD10, S100A4, α-SMA for CAFs, and Zeb1, Twist, and Slug in SCC, MM, and BCC and their associations with various clinicopathological factors, we used χ^2 tests, Kruskal-Wallis tests, and Mann-Whitney *U* tests with a 2 × 2 table to compare the categorical data. The level of significance was $P < .05$, and the confidence interval was determined at the 95% level. Statistical analyses were performed with the JMP 10.0 software package (SAS Institute, Inc) for Windows.

3. Results

Not only CAFs (fusiform cells) but also reactive interstitial cells (including inflammatory cells and histiocytes surrounding the invasive cancer cell nests) were observed in the invasive area. CAFs were considered fusiform or spindle shaped. Thus, we carefully excluded inflammatory cells, including histiocytes, from the examination.

We performed hierarchical clustering based on marker scores to evaluate differences in the expression patterns of CAF- and EMT-related markers in patients with SCC, MM, and BCC. Based on the expression patterns, 3 distinct immunohistologic subgroups emerged (Fig. 3). The vertical line shows the expression of each marker in fibroblasts, and the horizontal lines denote "relatedness" between samples.

3.1. Association of each subgroup with clinicopathological variables in BCC, SCC, and MM

Some clinicopathological variables were correlated with the expression pattern of CAF- and EMT-related proteins. Median tumor size was significantly smaller in tumors in subgroup 2 than those in subgroups 1 and 3. In histopathological diagnosis, there was a statistical difference in the frequency of BCC between subgroup 2 and subgroups 1 and 3. We also observed a significant difference in the frequency of SCC between subgroup 3 and subgroups 1 and 2. The frequency of MM was significantly higher in subgroup 1 than in subgroups 2 and 3. Overall, each subgroup that we examined was correlated with each histologic subtype. Next, although median tumor thickness was statistically lower in subgroup 2 than in subgroups 1 and 3, no association of any subgroup with the Clark level was found. Finally, there was a significant difference in the frequencies of lymph node metastases between subgroups 1 and 2. The association of each subgroup with its clinicopathological variables is depicted in Table 4.

3.2. Association of each subgroup with CAF- and EMT-related proteins in BCC, SCC, and MM

Comparisons of CAF- and EMT-related markers within subgroups 1, 2, and 3 were performed in those tumors with scores greater than 2. Each subgroup was defined by specific expression patterns of CAF- and EMT-related proteins. Subgroup 1 was characterized by low expression of AEBP1, PDGFRα, PDGFRβ, FAP, and Slug, whereas subgroup 2 was closely associated with high expression of PDGFRβ, S100A4, and Twist. In addition, high expression levels of

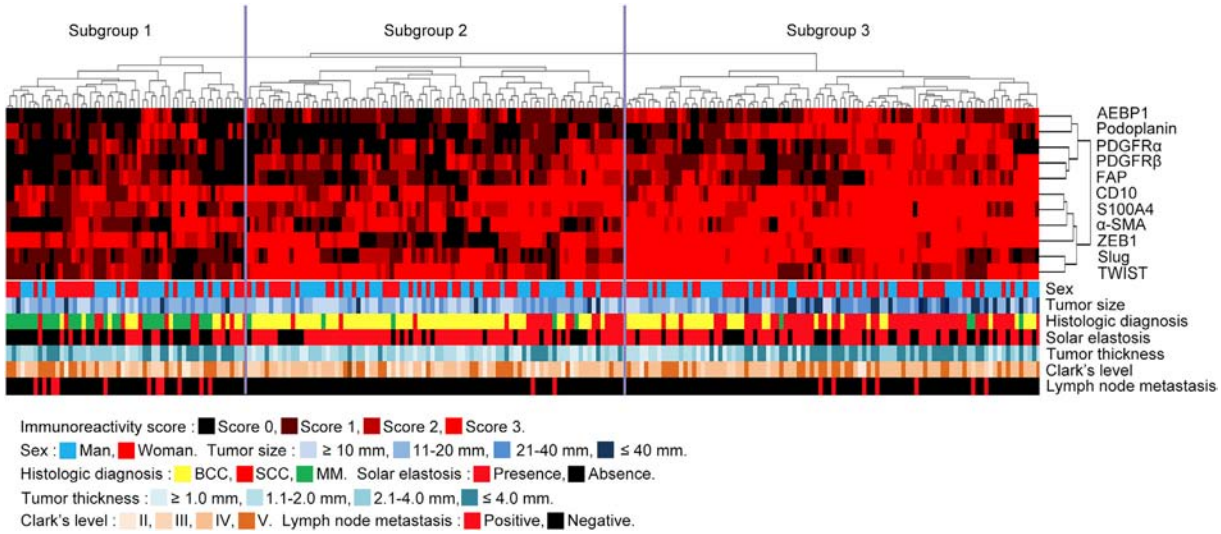

Fig. 3 Hierarchical cluster analysis of cutaneous cancers, including MM, BCC, and SCC, based on the protein expression patterns of CAF and the EMT. The cutaneous cancers were classified into 3 subgroups.

Table 4 Clinicopathological variables in subgroups 1, 2, and 3

	Subgroup 1	Subgroup 2	Subgroup 3	*P*
No. cases (%)	55 (23.0)	87 (37.0)	95 (40.0)	
Sex (man/woman)	27/28	41/46	41/54	NS
Tumor size (mm), median (range)	20.0 (1.5-50.0) [a,b]	13.0 (1.5-70.0) [a,b]	22.5 (6.0-140.0) [b]	*P* < .0001
Histologic classification (%)				*P* < .0001
BCC	12 (21.8) [b]	63 (72.4) [b]	35 (36.8) [b]	
SCC	12 (21.8) [b]	19 (21.8) [b]	56 (58.9) [b]	
MM	31 (56.4) [b]	5 (5.7) [b]	4 (4.2) [b]	
Solar elastosis (%)				*P* = .0003
Presence	22 (40.0) [b, c]	64 (73.5) [b]	61 (64.2) [c]	
Absence	33 (60.0)	23 (26.4)	34 (35.8)	
Tumor thickness (mm), median (range)	3.5 (1.0-13.5) [b]	1.8 (0.3-10.5) [b]	3.0 (0.2-24.5) [b]	*P* < .0001
Clark's level (%)				NS
II	5 (9.0)	10 (11.5)	3 (3.2)	
III	10 (18.2)	16 (18.4)	7 (7.3)	
IV	20 (36.4)	44 (50.6)	55 (57.9)	
V	20 (36.4)	17 (19.5)	30 (31.6)	
Lymph node metastasis, positive (%)	11 (20.0) [d]	2 (2.29) [d]	7 (7.29)	*P* = .0010

[a] *P* = .0119.
[b] *P* < .0001.
[c] *P* = .0041.
[d] *P* = .0004.

podoplanin, PDGFRβ, CD10, S100A4, α-SMA, Zeb1, Slug, and Twist were observed in subgroup 3. High expression of CD10 was commonly found in subgroups 1, 2, and 3. The association of each subgroup with individual markers is shown in Fig. 4.

4. Discussion

No previous study has reported associations between common skin tumors (BCC, SCC, and MM) and the expression patterns of CAF- and EMT-related proteins. The stromal features are expected to be different because different clinicopathological findings have been observed among the tumors. Traditionally, the prediction of tumor behavior has been associated with cancer cells per se. It is now apparent that stromal cells surrounding the cancer nest play a crucial role in the tumor's progression and metastasis [12]. Recent studies have identified many aspects of tumor-stroma interactions [19]. Surprisingly, interstitial cells can be beneficial to the cancer cells [12,19]. In the present study, we focused on CAFs surrounding invasive cancer nests in BCC, SCC, and MM.

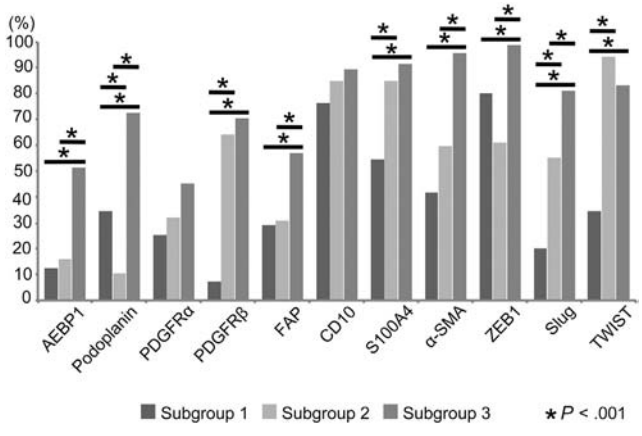

Fig. 4 Comparison of CAF- and EMT-related markers for each subgroup in tumors with scores greater than 2.

To identify the role of expressed CAF-related proteins, we used 8 markers that are closely associated with CAFs (AEBP1, podoplanin, PDGFRα, PDGFRβ, FAP, CD10, S100A4, and α-SMA). AEBP1 was reported to be a unique protein that functions as an important regulator of adipose tissue homeostasis [20,21]. Nonetheless, we suggest that AEBP1 is also a new CAF marker, given that it was expressed in CAFs. Podoplanin is expressed in the lymphatic endothelium. However, podoplanin is also a representative CAF-related marker [22,23]. Although PDGF signaling in tumor cells is activated by point mutations, amplification [24,25], and translocations, the mechanism that induces PDGFRα and PDGFRβ in CAFs remains unknown. The desmoplastic response that is frequently observed at the invasive front seems to be mediated by PDGFRα and PDGFRβ signaling in CAFs [24,25]. It is thought that PDGFRα and PDGFRβ are reliable markers for CAFs [24,25]. Recent study has shown that stromal Gremlin 1 (*GREM1*) expression is linked to CAFs where its expression

is strongly correlated with that of CD10 at the invasion front of BCC [26]. CD10 is also a good marker for CAFs [27]. S100A4, a commonly used marker for CAFs, was elevated in the CAFs [28]. In previous studies, expression of S100A4 by CAFs was found to predict patient prognosis in some types of cancers [29,30]. FAP is a protein that is characteristically expressed by CAFs and is found in 90% of internal epithelial cancers and cutaneous epithelial malignancies [31]. α-SMA is a representative marker that defines CAFs in invasive cancer areas and is commonly observed in most types of cancer [26]. Accordingly, we believe that these 8 CAF-related markers are suitable for assessment of CAF in cutaneous malignant tumors.

It has been suggested that although down-regulation of E-cadherin at the invasive cancer front is induced by the aberrant expression of several transcriptional repressors including Zeb1, Slug, and Twist [13,15], their inhibitory roles and clinical importance are not yet well established in cutaneous cancers. These EMT-related proteins could also be expressed by CAFs. Thus, we included 3 CAF markers (Zeb1, Slug, and Twist) in the present study.

Activated CAFs and the EMT are now believed to promote tumor progression and to reduce patient survival [6-8]. In the present study, we categorized 3 types of cutaneous malignant tumors (MM and BCC, SCC) into 3 subgroups stratified by their expression pattern of CAF-related proteins and EMT-related proteins (the CAF phenotype). Tumors in subgroup 1 were characterized by low expression of AEBP1, PDGFRα, PDGFRβ, FAP, and Slug. In contrast, tumors in subgroup 3 were defined by up-regulation of podoplanin, PDGFRβ, CD10, S100A4, α-SMA, Zeb1, Slug, and Twist. Tumors in subgroup 2 were characterized by high expression of PDGFRβ, CD10, S100A4, and Twist. Finally, up-regulation of CD10 was a common finding in BCC, SCC, and MM we examined. Overall, tumors in subgroup 1 were characterized by low activity of CAF- and EMT-related proteins, whereas tumors in subgroups 2 and 3 were closely associated with high activity of CAF- and EMT-related proteins. These findings show that CAFs include heterogeneous populations of cells as reflected by their different phenotypes, suggesting the plasticity of CAFs. Taken together, the microenvironment at the tumor invasive front shows several specific expression patterns of CAF- and EMT-related proteins in cutaneous malignant tumors, including BCC, SCC, and MM.

In previous studies, the cancer cells were found to have different alterations and undergo different pathologic courses [3-5]. If so, one might predict that the CAFs and the EMTs might also vary in their different histologic subtypes. In the present study, a specific histologic type was indeed correlated with each subgroup that was stratified by cluster analysis. Thus, different CAF phenotypes were characteristic of BCC, SCC, and MM. This is the first report to show that the CAF phenotype plays an important role in the association between protein expression level and tumor type.

It is well accepted that lymph node metastasis of cancer influences patient outcome in cutaneous malignant tumors, including BCC, SCC, and MM [32-34]. Although the frequency of lymph node metastasis is known to be low in cutaneous BCC [33], it is high in cutaneous MM and SCC [32,34]. In the present study, the frequency of lymph node metastasis was significantly higher in tumors in subgroup 1 than in tumors in subgroups 2 and 3. This finding suggests that the expression patterns of CAF- and EMT-related markers play some role in the progression of MM. At this point, the underlying significance of the association between MM and the markers of subgroup 1 is not clear. However, the expression pattern of CAF- and EMT-related markers may be useful in the prediction of lymph node metastasis.

There are some limitations in the present study. First, we were unable to demonstrate an association of the 3 subgroups with patient prognosis. However, it is well known that the frequency of lymph node metastasis is very low in cutaneous BCC compared with MM [33]. Therefore, it is very difficult to determine whether the expression pattern of CAF- and EMT-related markers is useful for the prediction of patient prognosis in cutaneous malignant tumors. To clarify the utility of the biomarkers, a much larger study will be needed. Next, it is possible that the selection criteria used for CAF- and EMT-related markers were not optimal. However, we believe that those markers are indeed suitable for examining the role of CAF- and EMT-related proteins in cutaneous malignant tumors.

In conclusion, 3 distinct subgroups were defined by a combined analysis of CAF- and EMT-related proteins in BCC, SCC, and MM. Our results suggest that these tumors possess distinct and specific expression patterns of CAF- and EMT-related proteins. That is, subgroup 1 is best represented by MM, subgroup 2 is primarily constituted by BCC, and subgroup 3 is predominately SCC. Furthermore, we suggest that there may be different CAF phenotypes for each histologic type, such as BCC, SCC, and MM. Finally, the role of the different CAF phenotypes in each cutaneous cancer remains unclear. However, we suggest that the expression pattern of CAF- and EMT-related proteins (CAF phenotype) plays a crucial role in the formation of the tumor microenvironment and its contribution to tumor invasiveness and metastasis.

Acknowledgments

We gratefully acknowledge the technical assistance of members of the Department of Molecular Diagnostic Pathology, Iwate Medical University for their support.

Statement of author contributions

K. Sasaki, who is the first author, constructed the figures and tables and performed statistical analyses. T. Sugai, who is the corresponding author, contributed to the preparation of the manuscript and all aspects of data collection and analysis.

K. Ishida performed histologic diagnosis. H. Amano and M. Sakuraba provided input during the preparation of the manuscript. K. Kashiwa and S. Kobayashii assisted with clinical data and experiments.

Human rights statement and informed consent

All procedures were performed in accordance with the ethical standards of the Iwate Medical University and with the Declaration of Helsinki. Substitute for informed consent (approval by the institutional review board of Iwate Medical University) was obtained from all patients included in the study.

References

[1] Rangwala S, Tsai KY. Roles of the immune system in skin cancer. Br J Dermatol 2011;165:953-65.
[2] Feller L, Khammissa RAG, Kramer B, et al. Basal cell carcinoma, squamous cell carcinoma and melanoma of the head and face. Head Face Med 2016;12:11.
[3] Li YY, Hanna GJ, Laga AC, et al. Genomic analysis of metastatic cutaneous squamous cell carcinoma. Clin Cancer Res 2015;21:1447-56.
[4] Hutchin ME, Kariapper MS, Grachtchouk M, et al. Sustained Hedgehog signaling is required for basal cell carcinoma proliferation and survival: conditional skin tumorigenesis recapitulates the hair growth cycle. Genes Dev 2005;19:214-23.
[5] Inamdar GS, Madhunapantula SV, Robertson GP. Targeting the MAPK pathway in melanoma: why some approaches succeed and other fail. Biochem Pharmacol 2010;80:624-37.
[6] Li H, Fan X, Houghton J. Tumor microenvironment: the role of the tumor stroma in cancer. J Cell Biochem 2007;101:805-15.
[7] Omland SH, Wettergren EE, Mourier T, et al. Cancer associated fibroblasts (CAFs) are activated in cutaneous basal cell carcinoma and in the peritumoural skin. BMC Cancer 2017;17:675-83.
[8] Zhou B, Chen WL, Wang YY, et al. A role for cancer-associated fibroblasts in inducing the epithelial-to-mesenchymal transition in human tongue squamous cell carcinoma. J Oral Pathol Med 2014;43:585-92.
[9] El Khoury J, Kurban M, Kibbi AG, Abbas O. Fibroblast-activation protein: valuable marker of cutaneous epithelial malignancy. Arch Dermatol Res 2014;306:359-65.
[10] Bussard KM, Mutkus L, Stumpf K, et al. Tumor-associated stromal cells as key contributors to the tumor microenvironment. Breast Cancer Res 2016;18:84-94.
[11] Augsten M. Cancer-associated fibroblasts as another polarized cell type of the tumor microenvironment. Front Oncol 2014;4:62-9.
[12] Quail DF, Joyce JA. Microenvironmental regulation of tumor progression and metastasis. Nat Med 2013;19:1423-37.
[13] Karlsson MC, Gonzalez SF, Welin J, et al. Epithelial-mesenchymal transition in cancer metastasis through the lymphatic system. Mol Oncol 2017;11:781-91.
[14] Lee SY, Jeong EK, Ju MK, et al. Induction of metastasis, cancer stem cell phenotype, and oncogenic metabolism in cancer cells by ionizing radiation. Mol Cancer 2017;16:10-34.
[15] Serrano-Gomez SJ, Maziveyi M, Alahari SK. Regulation of epithelial-mesenchymal transition through epigenetic and post-translational modifications. Mol Cancer 2016;15:18-31.
[16] Lamouille S, Xu J, Derynck R. Molecular mechanisms of epithelial-mesenchymal transition. Nat Rev Mol Cell Biol 2014;15:178-96.
[17] Yamada N, Sugai T, Eizuka M, et al. Tumor budding at the invasive front of colorectal cancer may not be associated with the epithelial-mesenchymal transition. Hum Pathol 2017;60:151-9.
[18] Sugai T, Sugimoto R, Habano W, et al. Genetic differences stratified by PCR-based microsatellite analysis in gastric intramucosal neoplasia. Gastric Cancer 2017;20:286-96.
[19] Shiga K, Hara M, Nagasaki T, et al. Cancer-associated fibroblasts: their characteristics and their roles in tumor growth. Cancers (Basel) 2015;7:2443-58.
[20] Cheon DJ, Tong Y, Sim MS, et al. A collagen-remodeling gene signature regulated by TGF-β signaling is associated with metastasis and poor survival in serous ovarian cancer. Clin Cancer Res 2014;20:711-23.
[21] Groessl M, Slany A, Bileck A, et al. Proteome profiling of breast cancer biopsies reveals a wound healing signature of cancer-associated fibroblasts. J Proteome Res 2014;13:4773-82.
[22] Wojciechowska-Zdrojowy M, Szepietowski JC, Matusiak Ł, et al. Expression of podoplanin in non-melanoma skin cancers and actinic keratosis. Anticancer Res 2016;36:1591-7.
[23] Ugorski M, Dziegiel P, Suchanski J. Podoplanin—a small glycoprotein with many faces. Am J Cancer Res 2016;6:370-86.
[24] Kartha VK, Stawski L, Han R, et al. PDGFRβ is a novel marker of stromal activation in oral squamous cell carcinomas. PLoS One 2016;11:e0154645.
[25] Watts TL, Cui R, Szaniszlo P, et al. PDGF-AA mediates mesenchymal stromal cell chemotaxis to the head and neck squamous cell carcinoma tumor microenvironment. J Transl Med 2016;14:337-46.
[26] Kim HS, Shin MS, Cheon MS, et al. GREM1 is expressed in the cancer-associated myofibroblasts of basal cell carcinomas. PLoS One 2017;12:e0174565.
[27] Yada K, Kashima K, Daa T, et al. Expression of CD10 in basal cell carcinoma. Am J Dermatopathol 2004;26:463-71.
[28] Rasanen K, Sriswasdi S, Valiga A, et al. Comparative secretome analysis of epithelial and mesenchymal subpopulations of head and neck squamous cell carcinoma identifies S100A4 as a potential therapeutic target. Mol Cell Proteomics 2013;12:3778-92.
[29] Yang X, Lin Y, Shi Y, et al. FAP promotes immunosuppression by cancer-associated fibroblasts in the tumor microenvironment via STAT3-CCL2 signaling. Cancer Res 2016;76:4124-35.
[30] Ha SY, Yeo SY, Xuan YH, et al. The prognostic significance of cancer-associated fibroblasts in esophageal squamous cell carcinoma. PLoS One 2014;9:e99955.
[31] Xing F, Saidou J, Watabe K. Cancer associated fibroblasts (CAFs) in tumor microenvironment. Front Biosci (Landmark Ed) 2010;15:166-79.
[32] Moore BA, Weber RS, Prieto V, et al. Lymph node metastases from cutaneous squamous cell carcinoma of the head and neck. Laryngoscope 2005;115:1561-7.
[33] Boswell JS, Flam MS, Tashjian DN, et al. Basal cell carcinoma metastatic to cervical lymph nodes and lungs. Dermatol Online J 2006;12:9-17.
[34] Zbytek B, Carlson JA, Granese J, et al. Current concepts of metastasis in melanoma. Expert Rev Dermatol 2008;3:569-85.